Effect of phase-conjugate feedback on the noise characteristics of semiconductor lasers

Govind P. Agrawal and George R. Gray
The Institute of Optics, University of Rochester, Rochester, New York 14627
(Received 18 March 1992)

This paper considers the effect of phase-conjugate feedback (PCF) on the noise characteristics of semiconductor lasers. By using the single-mode, rate-equation formalism, it is shown that semiconductor lasers can achieve a steady state as long as the amount of PCF is below a critical value. For an ideal phase-conjugate mirror, the average value of the steady-state phase of the semiconductor laser is found to be locked to a fixed value, determined by the linewidth-enhancement factor of the laser. The noise characteristics in the presence of PCF are studied by adding the Langevin-noise terms representing the effect of spontaneous emission to the rate equations and solving them approximately. Both the intensity noise and the frequency noise are reduced at low frequencies (below 100 MHz). In particular, the frequency noise nearly vanishes at zero frequency because of the phase-locked nature of the steady-state solution. The spectral line shape does not remain Lorentzian in the presence of PCF. The satellite peaks occurring at the relaxation-oscillation frequency are considerably enhanced because of a reduction in the damping rate of such oscillations.

PACS number(s): 42.55.Px, 42.60.Mi

I. INTRODUCTION

The noise characteristics of semiconductor lasers, such as the relative intensity noise (RIN) and the spectral linewidth, are known to be extremely sensitive to the optical feedback occurring when a portion of the laser output is fed back into the laser cavity after being reflected from an external reflecting surface [1,2]. Some unintentional feedback invariably occurs when semiconductor lasers are used in actual system applications. For example, feedback from the near and far ends of an optical fiber affects the performance of optical data links and lightwave communication systems unless optical isolators are used in between the laser and the fiber. Similarly, reflections from an optical disk affect the performance of optical recording systems. The effect of optical feedback on the semiconductor laser noise has been extensively studied [1–8]. It can be harmful for some applications since the feedback often enhances the RIN. On the other hand, optical feedback can be used to advantage, as it can reduce the laser linewidth with a proper design [3].

Recently considerable attention has been paid to the case in which optical feedback occurs as a result of reflection from a phase-conjugate mirror (PCM) [9–17]. Such a feedback is referred to as the phase-conjugate feedback (PCF) and differs considerably from the conventional-mirror feedback since the phase of the returned light is reversed during reflection. Several experiments have suggested that both the intensity and phase noise of a solitary laser may be reduced through PCF [9–15]. The problem does not appear to have attracted much attention theoretically. In a recent paper Agrawal and Klaus [17] considered the stability of semiconductor lasers in the presence of PCF and showed that the steady state can become unstable, leading to self-pulsing and chaos when the amount of PCF exceeds a critical value. In this paper we consider the stable regime and study how the intensity and phase noise of a semiconductor laser are affected by a small amount of PCF such that the laser continues to operate continuously (cw operation). We assume for simplicity that the PCF is provided by a perfect PCM that responds instantaneously without a change in the signal frequency. Degenerate four-wave mixing inside a fast nonlinear medium (response time less than 1 ps) pumped by a narrow-linewidth laser can provide a PCM whose performance approaches the ideal PCM assumed here.

In Sec. II, the rate equations for a semiconductor laser in the presence of PCF are given and the various parameters are described. In Sec. III, these rate equations are solved in the steady state, and the stability of the steady-state solutions is investigated. The laser's relative intensity noise as well as the frequency noise are calculated in Sec. IV, while the laser line shape is calculated in Sec. V. A discussion of these results, as well as conclusions, is presented in Sec. VI.

II. RATE EQUATIONS WITH PCF

The dynamical behavior of semiconductor lasers is generally modeled by a set of rate equations by assuming that the dipole relaxation time (T_2 in the terminology of two-level systems) is short enough that the gain medium is able to respond almost instantaneously to the changes in the optical field. In the presence of PCF, these equations can be written as (assuming single-mode operation) [1,2]

$$\frac{dE}{dt}=i\Delta\omega E(t)+\frac{1}{2}\left[G-\frac{1}{\tau_p}\right](1-i\alpha)E(t)+F_E(t)+\kappa E^*(t-\tau)\exp(i\phi_{\mathrm{PCM}}) , \quad (1)$$

$$\frac{dN}{dt}=\frac{I}{q}-\frac{N(t)}{\tau_e}-G(t)|E(t)|^2+F_N(t) , \quad (2)$$

where $E(t)$ is the slowly varying complex amplitude of the intracavity optical field, $\Delta\omega$ is the frequency shift from the threshold value, τ_p is the photon lifetime, α is the linewidth enhancement factor, N is the electron population, I is the injection current, q is the magnitude of the electron charge, τ_e is the electron lifetime, and G is the net rate of stimulated emission assumed to vary linearly with the electron population as

$$G = G_N(N - N_0) . \tag{3}$$

In Eq. (3), N_0 is the transparency value of N and the parameter G_N is related to the derivative of the optical gain with respect to the carrier density. The Langevin noise sources $F_E(t)$ and $F_N(t)$ represent the noise introduced by spontaneous emission and the shot noise due to carrier generation and recombination, respectively.

The last term in Eq. (1) is due to PCF and contains three parameters κ, τ, and ϕ_{PCM}. The feedback rate κ and the round-trip time τ are given by

$$\kappa = \frac{\eta_c(1-R_m)}{\tau_L}\left[\frac{R_{\text{PCM}}}{R_m}\right]^{1/2}, \quad \tau = \frac{2L_{\text{ext}}}{c} , \tag{4}$$

where η_c is the coupling efficiency, R_m is the laser facet reflectivity, τ_L is the round-trip time in the laser cavity, R_{PCM} is the reflectivity of the PCM, and L_{ext} is the spacing between the laser and the PCM. The parameter ϕ_{PCM} accounts for a constant phase shift occurring at the PCM. The round-trip phase shift $\omega_0\tau$, where ω_0 is the laser frequency, is absent in Eq. (1) because of the phase-conjugate nature of the feedback; i.e., any accumulated one-way phase shift gets canceled during the return trip. This feature introduces qualitative changes in the laser behavior in comparison with the case of conventional feedback. For example, the steady-state solutions of Eqs. (1) and (2) are independent of τ or the PCM location. Note, however, that the dynamic behavior still depends on τ because of the delayed nature of the feedback. Note also that the PCM is assumed to respond instantaneously in Eq. (1). If the PCM response is slower than the round-trip time τ, κ would become time dependent. This case can be studied by adding a third equation that governs the PCM dynamics to the set of Eqs. (1) and (2). Our approach assumes the PCM to be ideal. Such an ideal PCM cannot be realized by self-pumping. The assumptions implicit in this approach are that (i) the PCM is realized by using degenerate four-wave mixing in a fast-responding nonlinear medium, (ii) the pump frequency matches the semiconductor-laser frequency ω_0 exactly, and (iii) the pump beams are nearly monochromatic so that the noise induced by them can be ignored. The effect of pump noise can be included by adding pump-phase fluctuations to ϕ_{PCM}.

Equation (1) does not include the gain nonlinearities, which reduce G at high power levels. For this purpose, it is convenient to express $E(t)$ as

$$E(t) = \sqrt{P(t)}\exp[-i\phi(t)] , \tag{5}$$

where $P(t)$ is related to optical intensity and $\phi(t)$ is the optical phase. For simplicity of notation, $E(t)$ is assumed to be normalized such that $P(t)$ represents the number of photons stored in the laser cavity. By substituting Eq. (5) in Eq. (1), P and ϕ are found to satisfy the following two rate equations:

$$\frac{dP}{dt} = \left[G(1-\epsilon P) - \frac{1}{\tau_p}\right]P(t) + R_{\text{sp}} + F_P(t) + 2\kappa[P(t-\tau)P(t)]^{1/2}\cos[\phi(t)+\phi(t-\tau)+\phi_{\text{PCM}}] , \tag{6}$$

$$\frac{d\phi}{dt} = -\Delta\omega + \tfrac{1}{2}\alpha\left[G - \frac{1}{\tau_p}\right] + F_\phi(t) - \kappa\left[\frac{P(t-\tau)}{P(t)}\right]^{1/2}\sin[\phi(t)+\phi(t-\tau)+\phi_{\text{PCM}}] , \tag{7}$$

where G has been reduced by a power-dependent factor $1-\epsilon P$ in Eq. (6) to account for the gain reduction occurring because of the nonlinear nature of the gain [1]. The nonlinear-gain parameter ϵ controls the amount of gain reduction and has values $\sim 10^{-7}$. Since typically P is $\sim 10^5$, the gain reduction is at most by a few percent. The functional form of the nonlinear gain depends on the mechanism responsible for it and is generally different for the spectral hole-burning and carrier-heating mechanisms. However, in both cases the reduction factor can be written as $1-\epsilon P$ as long as $\epsilon P \ll 1$.

In Eqs. (6) and (7) R_{sp} represents the rate of spontaneous emission into the lasing mode, and $F_P(t)$ and $F_\phi(t)$ account for the noise by spontaneous emission. The effect of spontaneous emission is included in Eq. (1) through the Langevin noise source $F_E(t)$, a random quantity whose average vanishes. In the Markoffian approximation, the autocorrelation of $F_E(t)$ can be written as

$$\langle F_E(t)F_E^*(t')\rangle = R_{\text{sp}}\delta(t-t') , \tag{8}$$

where $\delta(t-t')$ is the Dirac delta function. The Langevin noise sources $F_P(t)$, $F_N(t)$, and $F_\phi(t)$ are also defined such that they vanish on average, i.e., $\langle F_i(t)\rangle = 0$ for $i = P$, N, and ϕ. Their second-order moments are δ-function correlated as

$$\langle F_i(t)F_j(t')\rangle = 2D_{ij}\delta(t-t') , \tag{9}$$

where D_{ij} is the diffusion coefficient and $i,j = P$, N, or ϕ. The explicit expressions for the diffusion coefficients are [1]

$$D_{PP} = R_{\text{sp}}P, \quad D_{\phi\phi} = R_{\text{sp}}/4P, \quad D_{P\phi} = 0 , \tag{10a}$$

$$D_{NN} = R_{\text{sp}} + N/\tau_e, \quad D_{PN} = -R_{\text{sp}}P, \quad D_{N\phi} = 0 . \tag{10b}$$

III. STEADY-STATE SOLUTION

The steady-state solution of Eqs. (2), (6), and (7) is obtained by neglecting the Langevin noise sources and setting the time derivatives to zero. Since Eqs. (6) and (7) explicitly contain the laser phase ϕ, the steady state can be reached only if ϕ becomes a constant, i.e., the laser phase is pinned. This is a consequence of the phase-conjugate nature of the feedback. The steady-state values of P and N are obtained by solving

$$[G(1-\epsilon P)-\tau_p^{-1}]P+R_{\rm sp}+2\kappa P\cos[2\phi+\phi_{\rm PCM}]=0 , \tag{11a}$$

$$\frac{I}{q}-\frac{N}{\tau_e}-GP=0 . \tag{11b}$$

By substituting $G-\tau_p^{-1}$ from Eq. (11a) into Eq. (7), the phase equation can be written as

$$\frac{d\phi}{dt}=-\Delta\omega+\Delta\omega_c-\kappa(1+\alpha^2)^{1/2}\sin(2\phi+\phi_{\rm PCM}+\phi_R) , \tag{12}$$

where

$$\phi_R=\tan^{-1}\alpha , \tag{13}$$

and $\Delta\omega_c$ is the static frequency chirp given by

$$\Delta\omega_c=\frac{\alpha}{2}(\epsilon GP-R_{\rm sp}/P) . \tag{14}$$

The dominant contribution to $\Delta\omega_c$ comes from the nonlinear gain.

In the absence of feedback ($\kappa=0$), Eq. (12) shows that the steady state can be reached if $\Delta\omega=\Delta\omega_c$. Thus the mode frequency shifts by $\Delta\omega_c$, a phenomenon known as mode pulling in laser theory. In the presence of feedback, this steady state can still be achieved if the laser phase ϕ is pinned to a value such that

$$2\phi+\phi_{\rm PCM}+\phi_R=2m\pi , \tag{15}$$

where m is an integer. The pinning of the laser phase ϕ to a constant value is a consequence of the phase-conjugate nature of the feedback. In the case of conventional feedback, ϕ does not appear in the steady-state phase equation. Rather, one obtains multiple solutions for the frequency shift $\Delta\omega$. In the case of PCF, the laser frequency remains unchanged and, at the same time, the laser phase ϕ gets pinned to a value specified by Eq. (15). It should be stressed that it is only the average phase that takes a constant value. Because of spontaneous emission, the actual phase ϕ fluctuates around its average value. However, as shown later, the character of phase fluctuations is also affected by the phase-conjugate nature of the feedback.

The stability of the phase-locked solution can be checked by linearizing Eqs. (2), (6), and (7) around the steady-state solution and solving the resulting set of three linear equations for the damping rate λ of small perturbations from the steady-state values. This standard procedure provides a third-order polynomial in λ as

$$D(\lambda)=C_3\lambda^3+C_2\lambda^2+C_1\lambda+C_0 , \tag{16}$$

where

$$C_3=1-a^2-b^2 , \tag{17a}$$

$$C_2=\Gamma_N(1-a^2-b^2)+\Gamma_P(1-a)+\frac{2}{\tau}(a+a^2+b^2) , \tag{17b}$$

$$C_1=\frac{2a\Gamma_P}{\tau}+\Gamma_N\left[\Gamma_P(1-a)+\frac{2}{\tau}(a+a^2+b^2)\right]+(1-a-\alpha b)GG_NP , \tag{17c}$$

$$C_0=\frac{2a}{\tau}\Gamma_P\Gamma_N+\frac{2}{\tau}(a-\alpha b)GG_NP . \tag{17d}$$

The parameters a, b, Γ_P, and Γ_N are defined as

$$a=\kappa\tau\cos(2\phi+\phi_{\rm PCM}),\quad b=\kappa\tau\sin(2\phi+\phi_{\rm PCM}) , \tag{18}$$

$$\Gamma_P=R_{\rm sp}/P+\epsilon GP,\quad \Gamma_N=1/\tau_e+G_NP . \tag{19}$$

The steady state becomes unstable whenever $\mathrm{Re}(\lambda)>0$ for any of the roots of the polynomial. Among the three roots, one root is real while the other two form a complex-conjugate pair. The real part of the complex-conjugate pair is related to the damping rate Γ_R of relaxation oscillations, while the imaginary part provides the frequency Ω_R of relaxation oscillations. Figure 1 shows how the damping rate Γ_R changes with feedback for the case in which $L_{\rm ext}=5$ cm ($\tau=0.33$ ns). Table I shows the values of device parameters used for numerical calculations. For $\kappa\tau=0$, the damping rate of a solitary laser is given by $\Gamma_R=(\Gamma_N+\Gamma_P)/2$, where Γ_N and Γ_P are obtained from Eq. (19). The effect of PCF is to reduce the damping rate such that Γ_R becomes zero at a certain value κ_c of the feedback parameter κ. The exact value of κ_c at which Γ_R becomes zero depends on the linewidth enhancement factor α. Qualitatively speaking, the critical value of κ_c decreases with an increase in α, as seen

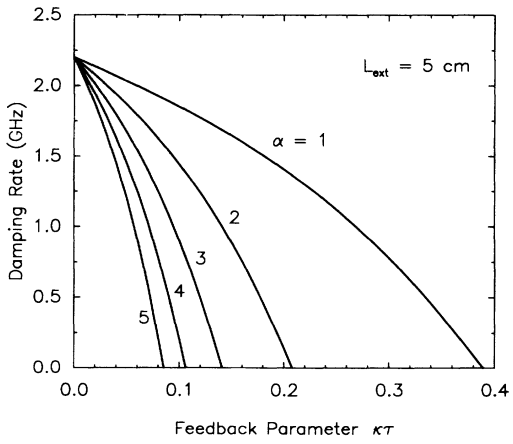

FIG. 1. Relaxation-oscillation damping rate Γ_R as a function of feedback strength $\kappa\tau$ for different values of α. The external cavity length is 5 cm ($\tau=0.33$ ns) and other parameter values are given in Table I.

clearly in Fig. 1. Since $\mathrm{Re}(\lambda)>0$ for $\kappa>\kappa_c$, the steady state becomes unstable through a Hopf bifurcation when the feedback level exceeds a critical level [17]. One can use Eq. (4) to estimate the phase-conjugate reflectively R_{PCM} for which κ exceeds κ_c. The coupling loss is expected to be negligible ($\eta_c \approx 1$) for PCF since the reflected light more or less traces the path of the emitted light. The laser-cavity round-trip time τ_L is about 6 ps for a 250-μm long cavity. If we take $R_m=30\%$ for the laser facet, assumed to be uncoated, $\kappa \approx 1\times10^9\ \mathrm{s}^{-1}$ for $R_{\mathrm{PCM}} \approx 2\times10^{-5}$. Clearly, the steady state can become unstable for relatively small levels of the PCF.

Even though the steady state does not depend on the external cavity length L_{ext}, the stability range depends on it because of the appearance of the feedback delay time τ in Eqs. (6) and (7). Figure 2 shows the variation of the critical value κ_c of the feedback parameter κ with L_{ext} by using the parameter values of Table I. The steady state for a given value of α is stable in the region below the curve corresponding to that value of α. In general, larger values of κ can be tolerated for smaller values of L_{ext}. However, the difference is relatively minor for large values of α. For $\alpha>2$, the feedback rate κ should be below 1 GHz for the steady state to remain stable. As noted earlier, such values of κ correspond to relatively small values of the feedback ($R_{\mathrm{PCM}} \lesssim 2\times10^{-5}$) for typical device parameters. It should be mentioned that the stability curves of Fig. 2 are sensitive to the exact values of the parameters. In particular, larger values of κ can be tolerated if the damping rate Γ_R of the solitary laser is larger. Since the dominant contribution to Γ_R comes from the nonlinear gain term in Eq. (19), κ_c would be larger for lasers for which ϵ is larger. Thus, $\mathrm{In}_{1-x}\mathrm{Ga}_x\mathrm{As}_y\mathrm{P}_{1-y}$ lasers may remain stable over a larger range of R_{PCM} than GaAs lasers for the same value of α. In practice, α is typically larger for $\mathrm{In}_{1-x}\mathrm{Ga}_x\mathrm{As}_y\mathrm{P}_{1-y}$ lasers, making them more sensitive to the PCF. Strained quantum-well lasers are expected to exhibit a much larger stability range, as α can be quite small for such devices

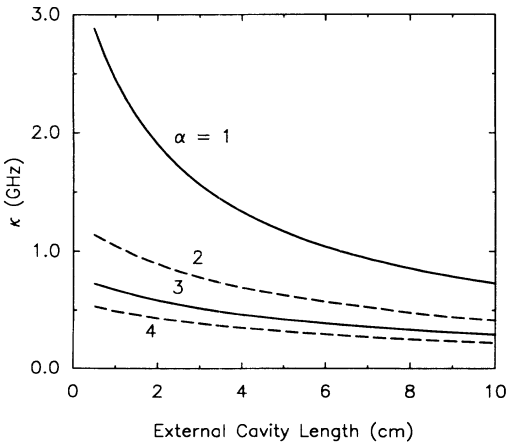

FIG. 2. Critical value of feedback parameter κ vs L_{ext} for different values of α. For a given value of α, the laser is stable in the region below the corresponding curve.

TABLE I. Parameters and their numerical values for a GaAs semiconductor laser operating at 5 mW.

Parameter	Symbol	Value
Photon lifetime	τ_p	1.5 ps
Electron lifetime	τ_e	2 ns
Gain coefficient	G_N	$4.5\times10^3\ \mathrm{s}^{-1}$
Rate of stimulated emission	G	$6.67\times10^{11}\ \mathrm{s}^{-1}$
Rate of spontaneous emission	R_{sp}	1.7 G
Number of photons per milliwatt		2.5×10^4
Operating output power	P_{out}	5 mW
Nonlinear gain coefficient	ϵ	4×10^{-8}
Linewidth-enhancement factor	α	3

($\alpha<1$ is possible in some cases), while, at the same time, ϵ is relatively large.

IV. INTENSITY AND FREQUENCY NOISE

To study the effect of PCF on the noise characteristics of semiconductor lasers, we need to solve Eqs. (2), (6), and (7), which include fluctuations in P, N, and ϕ through the Langevin noise sources. These equations generally require a numerical solution because of their nonlinear nature. However, it is possible to obtain an approximate analytic solution by linearizing these equations around the average steady-state values. The linearization procedure is generally valid for lasers operating far above the threshold, since fluctuations from the average values are relatively small in that case. Although we have solved Eqs. (2), (6), and (7) numerically, we follow the analytic approach in this paper because of the physical insight provided by it. Numerical results are in agreement with the analytical results for lasers operating far above threshold such that the output power exceeds a few milliwatts.

If p, n, and δ represent fluctuations from the steady-state average values of P, N, and ϕ, Eqs. (2), (6), and (7) lead to the following set of coupled linear equations after keeping terms up to first order in p, n, and δ:

$$(1+a)\dot{p}-2Pb\dot{\delta}=G_NPn-\Gamma_Pp-4(b/\tau)P\delta+F_p(t)\ , \tag{20}$$

$$(1-a)\dot{\delta}-(b/2P)\dot{p}=(\alpha/2)G_Nn-2(a/\tau)\delta+F_\phi(t)\ , \tag{21}$$

$$\dot{n}=-\Gamma_Nn-Gp+F_N(t)\ , \tag{22}$$

where a and b are given by Eq. (18) and Γ_P and Γ_N are given by Eq. (19). The delayed nature of the feedback was accounted for by approximating $P(t-\tau)$ and $\phi(t-\tau)$ by

$$P(t-\tau)=P(t)-\tau\dot{p}(t),\quad \phi(t-\tau)=\phi(t)-\tau\dot{\delta}\ . \tag{23}$$

This approximation has also been made in the previous work related to the conventional feedback and simplifies

the analysis considerably [3]. It is valid as long as p and ϕ vary slowly during the time interval τ so that $\tau\dot{p}(t)/p \ll 1$ and $\tau\dot{\delta}/\phi \ll 1$. This assumption is expected to hold if τ is less than the coherence time of the solitary laser.

Equations (20)–(22) can be solved in the Fourier domain in a straightforward manner owing to their linear nature. Thus, by using

$$p(t)=\frac{1}{2\pi}\int_{-\infty}^{\infty}\tilde{p}(\omega)\exp(i\omega t)d\omega\ , \tag{24}$$

and similar relations for $n(t)$, $\delta(t)$, $F_P(t)$, $F_\phi(t)$, and $F_N(t)$, we obtain the solution

$$\tilde{p}(\omega)=\frac{1}{\Delta}\left[a_{22}\left[\tilde{F}_P+\frac{G_N P\tilde{F}_N}{\Gamma_N+i\omega}\right]-a_{12}\left[\tilde{F}_\phi+\frac{\alpha}{2}\frac{G_N\tilde{F}_N}{\Gamma_N+i\omega}\right]\right], \tag{25}$$

$$\tilde{\delta}(\omega)=\frac{1}{\Delta}\left[a_{11}\left[\tilde{F}_\phi+\frac{\alpha}{2}\frac{G_N\tilde{F}_N}{\Gamma_N+i\omega}\right]-a_{21}\left[\tilde{F}_P+\frac{G_N P\tilde{F}_N}{\Gamma_N+i\omega}\right]\right], \tag{26}$$

$$\tilde{n}(\omega)=\frac{\tilde{F}_N-G\tilde{p}}{\Gamma_N+i\omega}\ , \tag{27}$$

where

$$a_{11}=[\Gamma_P+i\omega(1+a)](\Gamma_N+i\omega)+GG_N P\ , \tag{28a}$$

$$a_{12}=2bP(2/\tau-i\omega)(\Gamma_N+i\omega)\ , \tag{28b}$$

$$a_{21}=(\alpha/2)GG_N-i(b\omega/2P)(\Gamma_N+i\omega)\ , \tag{28c}$$

$$a_{22}=[2a/\tau+i\omega(1-a)](\Gamma_N+i\omega)\ , \tag{28d}$$

$$\Delta=(a_{11}a_{22}-a_{12}a_{21})/(\Gamma_N+i\omega)\ , \tag{29}$$

a and b are given by Eq. (18) and Γ_P and Γ_N are given by Eq. (19). The denominator Δ in Eqs. (25) and (26) is a third-degree polynomial in ω and is related to D appearing in Eq. (16) as $\Delta(\omega)=D(i\omega)$.

The spectrum of intensity and phase fluctuations is obtained by using Eqs. (25) and (26), which show how the Langevin noise sources $\tilde{F}_P$, $\tilde{F}_\phi$, and $\tilde{F}_N$ contribute to such fluctuations. It is common to characterize intensity fluctuations through the RIN spectrum and phase fluctuations through the frequency noise spectrum (FNS) defined as [1,2]

$$S_{\rm RIN}(\omega)=\langle|\tilde{p}(\omega)|^2\rangle/P^2\ , \tag{30}$$

$$S_{\rm FNS}(\omega)=\langle|\omega\tilde{\phi}(\omega)|^2\rangle\ . \tag{31}$$

The average over the Langevin noise sources can be performed by using Eqs. (9) and (10). The contribution of $\tilde{F}_N$ is generally negligible to both the RIN and the FNS. If we ignore this contribution for simplicity, RIN and FNS are found to be given by

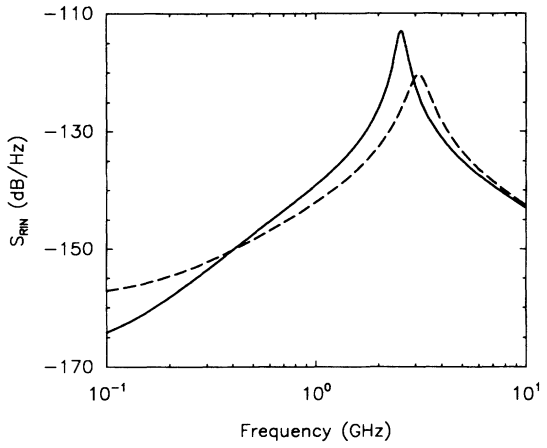

FIG. 3. RIN spectrum at 5 mW output power for $\kappa\tau=0.1$, $L_{\rm ext}=5$ cm, and $\alpha=3$. Dashed curve shows the RIN spectrum of the solitary laser ($\kappa\tau=0$).

$$S_{\rm RIN}(\omega)=\frac{2R_{\rm sp}}{P|\Delta|^2}\left[|a_{22}|^2+\frac{|a_{12}|^2}{4P^2}\right], \tag{32}$$

$$S_{\rm FNS}(\omega)=\frac{2\omega^2R_{\rm sp}P}{|\Delta|^2}\left[|a_{21}|^2+\frac{|a_{11}|^2}{4P^2}\right]. \tag{33}$$

Figures 3 and 4 show RIN and FNS for $\alpha=3$ for a laser operating at 5 mW when the PCF is such that $\kappa\tau=0.1$ and $L_{\rm ext}=5$ cm ($\tau=0.33$ ns). Dashed curves show for comparison the expected behavior in the absence of feedback. The RIN spectrum shows that the low-frequency RIN is reduced by the feedback, while the RIN is enhanced near the relaxation-oscillation frequency (which is slightly reduced from its solitary-laser value). The FNS shows a similar behavior, except that the frequency noise is reduced by orders of magnitudes at low frequencies. In fact, it is easy to show by taking the limit $\omega\to0$ in Eq. (33) that the spectral density of frequency

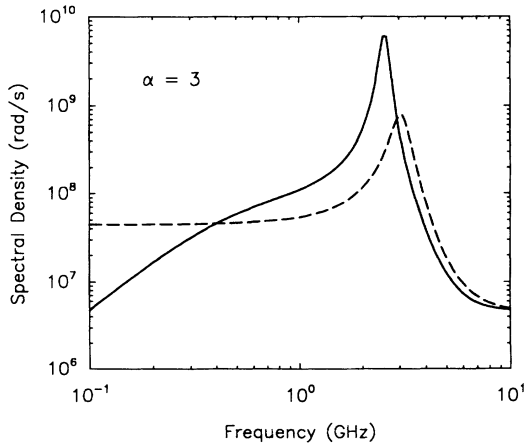

FIG. 4. FNS at 5 mW output power for $\kappa\tau=0.1$, $L_{\rm ext}=5$ cm, and $\alpha=3$. Dashed curve shows the FNS of the solitary laser ($\kappa\tau=0$).

noise vanishes at $\omega=0$. This is in sharp contrast with the solitary-laser FNS, which becomes flat at low frequencies and takes a constant nonzero value at $\omega=0$. The reason behind such a qualitative change can be understood by noting that the PCF locks the average value of the laser phase in the long-time limit. Since the frequency fluctuations are related to $d\phi/dt$, which becomes zero as $t\to\infty$, clearly the frequency noise vanishes as $\omega\to 0$. In practice, pump noise added by the PCM mirror would make it impossible to realize complete phase locking. The spectral density of frequency noise near $\omega=0$ would then not vanish but take a value that is governed by the linewidth of the pump laser. The next section considers the effect of PCF on the single-mode spectrum.

V. SPECTRAL LINE SHAPE

The spectral line shape is obtained by taking the Fourier transform of the field autocorrelation and is given by

$$S_E(\omega)=\frac{1}{P}\mathrm{Re}\left[\int_0^\infty \langle E^*(t+t')E(t)\rangle \exp(-i\omega t')dt'\right], \tag{34}$$

where Re stands for the real part of the bracketed expression and the optical field $E(t)$ is given by

$$E(t)=[P+p(t)]^{1/2}\exp[-i(\phi+\delta(t))]\ . \tag{35}$$

The angular brackets denote the ensemble average over the intensity and phase fluctuations, denoted by $p(t)$ and $\delta(t)$ in Eq. (35). The effect of intensity fluctuations on the spectral line shape is almost negligible for lasers operating far above threshold. By substituting Eq. (35) into (34) and neglecting $p(t)$, we obtain

$$S_E(\omega)=\mathrm{Re}\left[\int_0^\infty \exp[-\tfrac{1}{2}\langle \Delta\phi^2(t')\rangle]\exp(-i\omega t')dt'\right], \tag{36}$$

where $\Delta\phi(t')=\delta(t+t')-\delta(t)$ is the difference in phase fluctuations at times $t+t'$ and t. In obtaining Eq. (36), $\Delta\phi(t')$ is assumed to be a Gaussian stochastic process, so that

$$\langle \exp[i\Delta\phi(t')]\rangle=\exp[-\tfrac{1}{2}\langle \Delta\phi^2(t')\rangle]\ . \tag{37}$$

By using the Fourier relation

$$\delta(t)=\frac{1}{2\pi}\int_{-\infty}^{\infty}\tilde{\delta}(\omega)\exp(i\omega t)d\omega\ , \tag{38}$$

the variance of $\Delta\phi(t')$ is found to be

$$\langle \Delta\phi^2(t')\rangle=\frac{1}{\pi}\int_{-\infty}^{\infty}\langle|\tilde{\delta}(\omega)|^2\rangle(1-\cos\omega t')d\omega\ , \tag{39}$$

where $\tilde{\delta}(\omega)$ is given by Eq. (26). Thus the spectral line shape is obtained in two steps. First, the phase variance is calculated by using Eq. (39). Second, the result is used in Eq. (36) to obtain $S_E(\omega)$.

To calculate the phase variance $\langle \Delta\phi^2(t')\rangle$, we substitute $\tilde{\delta}(\omega)$ from Eq. (26) into Eq. (39). For simplicity, we neglect the contribution of F_N to the laser spectrum. It can be included in a straightforward manner. The result is

$$\langle \Delta\phi^2(t')\rangle=\frac{R_{\mathrm{sp}}}{2\pi P}\int_{-\infty}^{\infty}(|a_{11}|^2+4P^2|a_{21}|^2)\times\frac{(1-\cos\omega t')}{|\Delta(\omega)|^2}d\omega\ . \tag{40}$$

This integral can be performed analytically by using the method of contour integration. The denominator $|\Delta(\omega)|^2$ is a sixth-order polynomial in ω with six roots given by $\pm i\lambda_1$, $\pm i\lambda_2$, and $\pm i\lambda_3$, where λ_1, λ_2, and λ_3 are the three roots of the third-degree polynomial $D(\lambda)$ given by Eq. (16). Since one root of $D(\lambda)$ is real (call it γ), $|\Delta(\omega)|^2$ has two zeros, $\pm i\gamma$, lying on the imaginary axis. The other four zeros lie at $\pm\Omega_R\pm i\Gamma_R$, where Ω_R and Γ_R are the frequency and the damping rate of relaxation oscillations. If we close the contour in the upper-half plane, only three poles (at $i\gamma$, $\Omega_R+i\Gamma_R$, and $-\Omega_R+i\Gamma_R$) contribute to the integral. The dominant contribution comes from the pole lying on the imaginary axis. If we retain only this contribution, the phase variance is given by

$$\langle \Delta\phi^2(t')\rangle=\frac{R_{\mathrm{sp}}}{2P}(|a_{11}|^2+4P^2|a_{21}|^2)\times\frac{1-\exp(-\gamma t)}{\gamma[(\Gamma_R-\gamma)^2+\Omega_R^2]^2}\ , \tag{41}$$

where a_{11} and a_{21} are evaluated at $\omega=i\gamma$.

Figure 5 shows the phase variance calculated by using the parameter values of Table I for several values of $\kappa\tau$. The external cavity length of 5 cm corresponds to $\tau=0.33$ ns. The contribution of all three poles was included in Fig. 5. Oscillations seen near the origin are due to relaxation oscillations and result from the contribution of poles located at $\Omega_R\pm i\Gamma_R$. This contribution vanishes after a few nanoseconds, after which $\langle \Delta\phi^2(t')\rangle$ is given by Eq. (41). Figure 5 shows the dramatic change introduced by the phase-conjugate nature of the feedback. For a solitary laser ($\kappa=0$), $\langle \Delta\phi^2(t')\rangle$ varies linearly with

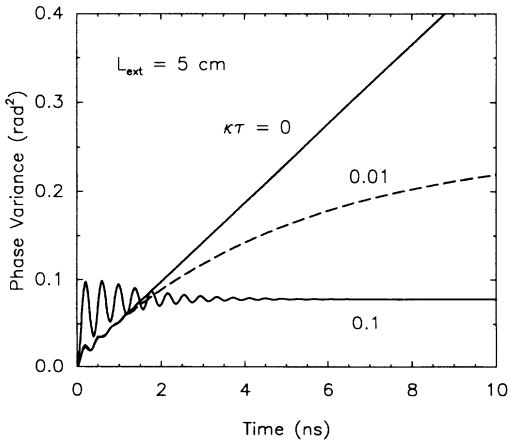

FIG. 5. Phase variance $\langle \Delta\phi^2\rangle$ as a function of time for several values of $\kappa\tau$ with $\alpha=3$. The saturation of $\langle \Delta\phi^2\rangle$ at long times is a consequence of the phase-locking nature of the PCF.

time. Indeed, $\gamma=0$ when $\kappa=0$, and Eq. (41) shows that $\langle\Delta\phi^2(t')\rangle$ increases linearly with time, as expected. This linear dependence is preserved when the feedback originates from a conventional mirror since $\gamma=0$ remains a root of the polynomial $D(\lambda)$ in Eq. (16). However, γ becomes nonzero in the case of PCF. Equation (41) shows that $\langle\Delta\phi^2(t')\rangle$ then saturates to a constant value after a time such that $t\gg\gamma^{-1}$. Physically, saturation of phase variance is a consequence of phase locking discussed in Sec. III in the context of the steady-state solutions.

The line shape is calculated by substituting phase variance $\langle\Delta\phi^2\rangle$ into Eq. (36) and evaluating the integral. In general, a numerical evaluation of this integral is necessary by using the fast-Fourier-transform (FFT) algorithm. However, physical insight is gained by considering again the poles of $|\Delta|^2$. The dominant contribution to the line shape comes from the pole $i\gamma$ lying at the imaginary axis. This pole results in a central peak, while the poles at $-\Omega_R+i\Gamma_R$ and $\Omega_R+i\Gamma_R$ result in satellite peaks located at multiples of Ω_R. Consider first the effect of PCF on the central peak. For this purpose we substitute $\langle\Delta\phi^2\rangle$ from Eq. (41) in Eq. (36) and obtain

$$S_E(\omega)=\mathrm{Re}\left\{\int_0^\infty \exp\left[-\frac{\beta}{\gamma}(1-e^{-\gamma t})-i\omega t\right]dt\right\}, \tag{42}$$

where

$$\beta=\frac{R_{sp}}{4P}\frac{(|a_{11}|^2+4P^2|a_{21}|^2)}{[(\Gamma_R-\gamma)^2+\Omega_R^2]^2}\approx\frac{R_{sp}}{4P}(1+\alpha^2)\,. \tag{43}$$

The last approximation follows from Eq. (28) by noting that Ω_R^2 can be approximated by GG_NP in most practical cases and that Ω_R is much larger than other rates Γ_P, Γ_N, Γ_R, and γ. In the absence of feedback ($\kappa=0$), $\gamma=0$. The integral can then be performed analytically with the result

$$S_E(\omega)=\frac{\beta}{(\beta^2+\omega^2)}\,. \tag{44}$$

As expected, the lineshape is Lorentzian with a full width at half maximum (FWHM) given by

$$\Delta\nu=\frac{\beta}{\pi}=\frac{R_{sp}}{4\pi P}(1+\alpha^2)\,. \tag{45}$$

This is a well-known expression for the linewidth of a solitary laser.

The evaluation of the integral in Eq. (42) is not straightforward when γ becomes finite because of external feedback. It is easy to see that the integral diverges at $\omega=0$, since the integrand does not vanish as $t\to\infty$. This is a consequence of the saturation of $\langle\Delta\phi^2\rangle$ in Fig. 5. It turns out that the spectrum consists of a sharp spike (related to the saturation of $\langle\Delta\phi^2\rangle$ to a constant) superimposed on a broad pedestal (related to the short-time behavior of $\langle\Delta\phi^2\rangle$ as in Fig. 5). In order to make the integral well defined we multiply the integrand by $\exp(-\epsilon t)$ and take the limit $\epsilon\to0$ at the end. Equation (42) can then be written as

$$S_E(\omega)=\mathrm{Re}\left[\sum_{n=0}^{\infty}\frac{1}{n!}\left[\frac{-\beta}{\gamma}\right]^n\int_0^\infty(1-e^{-\gamma t})^n e^{-\mu t}dt\right], \tag{46}$$

where $\mu=\epsilon+i\omega$. The integral in Eq. (46) can be found in the tables of integrals [18] and can be written in terms of a β function as long as $\gamma>0$. If we express the β function in terms of the Γ functions [19], the result is

$$S_E(\omega)=\mathrm{Re}\left[\sum_{n=0}^{\infty}\left[\frac{-\beta}{\gamma}\right]^n\frac{\gamma^{-1}\Gamma(\mu/\gamma)}{\Gamma(n+1+\mu/\gamma)}\right]. \tag{47}$$

If we now use the identity [19]

$$\Gamma(n+1+z)=(n+z)(n-1+z)\cdots(1+z)z\Gamma(z)\,, \tag{48}$$

the final result is

$$S_E(\omega)=\mathrm{Re}\left[\sum_{n=0}^{\infty}\frac{(-\beta/\gamma)^n}{(n+\mu/\gamma)\cdots(1+\mu/\gamma)\mu}\right]. \tag{49}$$

This series can be readily summed to obtain the line shape for given values of β and γ. The parameter $\mu=\epsilon+i\omega$ is replaced by $i\omega$ when the limit $\epsilon\to0$ is taken. The spectrum remains well defined for all frequencies except near $\omega=0$ where a sharp spike exists.

Figure 6 shows the low-frequency portion of the line shape obtained by using Eq. (49) for several values of γ in the range 10–100 MHz. Such values of γ occur for the case of weak feedback such that κ is in the range $(10^6-10^8)\ \mathrm{s}^{-1}$. The parameter $\beta=\pi\Delta\nu$, and $\Delta\nu$ is chosen to be 20 MHz. In the absence of feedback ($\kappa=0$), the long-time behavior of $\langle\Delta\phi^2\rangle$ (since it is linear in time) leads to a line shape that is Lorentzian at low frequencies with a FWHM of 20 MHz. This case is shown for comparison by a dashed line in Fig. 6. As the PCF increases, $\langle\Delta\phi^2\rangle$ saturates at long times causing the Lorentzian spectrum to narrow and to develop a narrow spike riding on a pedestal whose width can be larger than $\Delta\nu$. The pedestal is narrower than $\Delta\nu$ at weak feedback levels

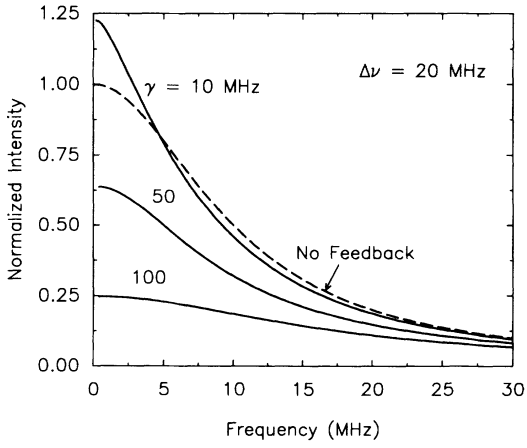

FIG. 6. Laser line shape in the low-frequency regime as obtained from Eq. (49) for different values of γ. Dashed curve shows the line shape of a solitary laser ($\gamma=0$ in the absence of PCF).

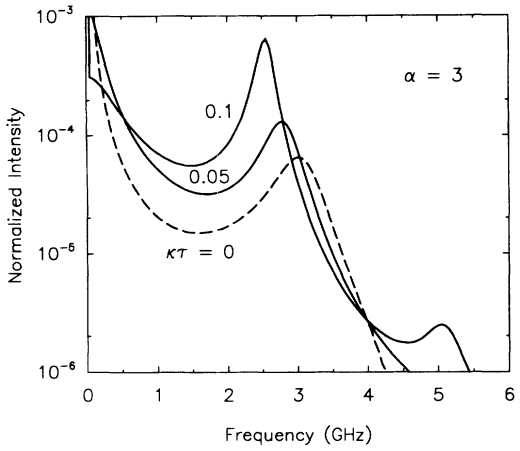

FIG. 7. Laser line shape evaluated numerically from Eq. (36) showing the effect of PCF on the laser relaxation oscillations. Dashed curve corresponds to the case of no feedback ($\kappa\tau=0$).

(10-MHz curve in Fig. 6) but becomes broader than $\Delta\nu$ at high feedback levels. In principle, the linewidth due to spontaneous emission is governed by the width of the narrow spike and nearly vanishes simply because the PCF locks the laser phase and saturates the phase variance. In practice, however, the narrow spike would be broadened by the presence of additional noise mechanisms (e.g., $1/f$ noise, pump noise, etc.), which we have neglected. The linewidth would then be determined by the width of the broadened spike. Since this width is expected to be less than the solitary-laser linewidth, the PCF would lead to line narrowing whose extent is governed by noise sources other than the spontaneous emission inside the laser cavity. The ultimate limit on linewidth reduction would be provided by the linewidth of the laser used to pump the PCM. An example of line narrowing (by a factor of 5) was provided in an experiment in which four-wave mixing in a semiconductor provided the PCF [15]. The effect of feedback on the linewidth is qualitatively different from the case of conventional feedback where the linewidth may increase or decrease depending on the round-trip phase shift in the external cavity.

The PCF is also expected to affect the satellite peaks occurring at the relaxation oscillation frequency Ω_R. Figure 7 shows the spectral line shape by evaluating Eq. (36) numerically through an FFT algorithm. The parameter values used were the same as those used for Fig. 5 and given in Table I. The satellite peak shifts toward shorter frequencies and its amplitude increases as the feedback level increases. This is easily understood by noting that the effect of feedback is to reduce both the frequency Ω_R and the damping rate of relaxation oscillation. At a critical value of the feedback level ($\kappa\tau=0.14$ for parameter values used here), the relaxation oscillations become undamped as Γ_R becomes zero. The amplitude of the satellite peaks then becomes comparable to the central peak. The growth of the satellite peaks implies that the steady state has become unstable, and the laser output is periodic with a repetition rate governed by Ω_R. Satellite peaks in that case correspond to the amplitude modulation sidebands expected for a periodic output.

VI. DISCUSSION AND CONCLUSION

This paper has studied the effect of PCF on the noise characteristics of semiconductor lasers. By using the rate equations, we have shown that the laser can achieve the steady state as long as the feedback level is below a critical value. The most important aspect of the steady state is that the average value of the optical phase ϕ is locked to a constant value governed by the linewidth enhancement factor and the phase shift occurring during reflection at the phase-conjugate mirror [see Eq. (15)]. Such a phase locking is expected to reduce the laser noise considerably. The results of Sec. IV show indeed that both the intensity noise and the frequency noise are considerably reduced at low frequencies. In fact, the frequency noise can nearly vanish at zero frequency (dc value of the frequency noise) because of the phase locking occurring in the long-time limit. This is in sharp contrast with the case of conventional feedback where the frequency noise is nearly uniform in the frequency range 0–1 GHz (white noise), although its magnitude is reduced for some values of the feedback parameters. Because of the nonuniformity of the frequency noise at low frequencies, the linewidth cannot be related to the dc value of the frequency noise. In fact, the line shape does not even remain Lorentzian. Our results show that the line shape is in the form of a narrow spike riding on a relatively broad pedestal, which contains the satellite peaks at multiples of the relaxation-oscillation frequency (enhanced in amplitude because of a reduction in the damping rate). In practice, additional noise mechanisms such as the pump noise and the $1/f$ noise [20] would determine the width of the narrow spike. In particular, the pump linewidth would provide the ultimate limit on the linewidth observed experimentally.

ACKNOWLEDGMENTS

This work is supported by the U.S. Army Research Office and the New York State Foundation of Science and Technology.

[1] G. P. Agrawal and N. K. Dutta, *Long-Wavelength Semiconductor Lasers* (Van Nostrand Reinhold, New York, 1986), Chap. 6.

[2] K. Petermann, *Laser Diode Modulation and Noise* (Kluwer Academic, Dordrecht, Netherlands, 1988), Chap. 9.

[3] G. P. Agrawal, IEEE J. Quantum. Electron. **QE-20**, 468 (1984).

[4] D. Lenstra, B. H. Verbeek, and A. J. den Boef, IEEE J. Quantum Electron. **QE-21**, 674 (1985).

[5] C. H. Henry and R. F. Kazarinov, IEEE J. Quantum Electron. **QE-22**, 294 (1986).

[6] R. W. Tkach and A. R. Chraplyvy, J. Lightwave Technol.

LT-4, 1665 (1986).
[7] N. Schunk and K. Petermann, IEEE J. Quantum Electron. **24**, 1252 (1988); IEEE Photon. Tech. Lett. **1**, 49 (1989).
[8] J. Mork, B. Tromborg, and J. Mark, IEEE J. Quantum Electron. **28**, 93 (1992), and references cited therein.
[9] K. Vahala, K. Kyuma, A. Yariv, S. Kwonk, M. Cronin-Golomb, and K. Y. Lau, Appl. Phys. Lett. **49**, 1563 (1986).
[10] M. Cronin-Golomb and A. Yariv, Opt. Lett. **11**, 455 (1986).
[11] R. R. Stephens, R. C. Lind, and C. R. Giuliano, Appl. Phys. Lett. **50**, 647 (1987).
[12] Y. Champagne, N. McCarthy, and R. Tremblay, IEEE J. Quantum Electron. **25**, 595 (1989).
[13] M. Segev, Y. Ophir, B. Fischer, and G. Eisenstein, Appl. Phys. Lett. **57**, 2523 (1990).
[14] N. McCarthy and D. Gay, Opt. Lett. **16**, 1006 (1991).
[15] M. Ohtsu, I. Koshishi, and Y. Teramuchi, Jpn. J. Appl. Phys. **29**, L2060 (1990).
[16] B. H. W. Hendriks, M. A. M. de Jong, and G. Nienhuis, Opt. Commun. **77**, 435 (1990).
[17] G. P. Agrawal and J. T. Klaus, Opt. Lett. **16**, 1325 (1991).
[18] *Tables of Integrals, Series, and Products,* edited by I. S. Gradshteyn and I. M. Ryzhik (Academic, New York, 1980).
[19] *Handbook of Mathematical Functions,* edited by M. Abramowitz and I. A. Stegun (Dover, New York, 1970).
[20] K. Kikuchi, Electron. Lett. **24**, 1001 (1988); IEEE J. Quantum Electron. **25**, 684 (1989).